JOURNAL OF CATALYSIS **174,** 65–71 (1998)
ARTICLE NO. CA971958

Decomposition of Acetate Groups on an Alumina-Supported Rhodium Catalyst

M. Bowker[1] and T. J. Cassidy

Catalysis Research Centre, Department of Chemistry, The University, Whiteknights Park, Reading RG6 6AD, United Kingdom

Received July 15, 1997; revised October 24, 1997; accepted October 24, 1997

The decomposition of adsorbed acetate groups on a 1% Rh/Al_2O_3 catalyst has been investigated by means of temperature-programmed desorption (TPD) at atmospheric pressure, in a microreactor fitted with an on-line mass spectrometer. Under certain conditions of catalyst pretreatment, the adsorbed acetate groups decompose autocatalytically in a process that has been described in the past as a "surface explosion." The phenomenon of surface explosions has been investigated by various groups and was generally considered to be confined to ultrahigh vacuum regimes using single crystals. It is found, however, that the explosive acetate decomposition reaction actually translates directly to real supported metal catalysts at atmospheric pressure. A description is given involving the influence of adsorbed oxygen and differentiated acetate adsorption sites on the metal, the support, and at the interface between the two. Surface migration of the acetate groups is also involved in determining the intensities of the various TPD peaks.

1. INTRODUCTION

A very desirable industrial process and one that has attracted considerable interest over the past two decades is the direct synthesis of higher oxygenates (C_2+) from synthesis gas. The ability of supported rhodium catalysts to selectively achieve this goal, albeit in very small yields, was first recognized in the mid-1970s. The study of adsorbates on catalysts is fundamental to the identification of reaction intermediates and mechanisms in general, and in this case in particular. There are many oxygenated species seen on rhodium during CO/H_2 exposure including: acyl CH_3CO, acetyl CH_3CHO, ethoxy CH_3CH_2O, acetate CH_3COO, and deoxyethyl CH_3CHOO species. Debate continues, however, as to which of the adsorbates is the actual reaction intermediate and which ones are spectator species (2–4).

The role of oxygenate intermediates in the synthesis of ethanol on rhodium has previously been reviewed by one of the authors (5). Adsorbed acetate groups were argued, by microreversibility, to be the most likely reaction intermediates and have also been proposed by others to be of importance (6–9). It was this that led us to study acetate species on a real supported rhodium catalyst. The objective of this study was to look at the mode of acetate decomposition using temperature-programmed desorption and to relate these findings to previous work on single crystal metal surfaces (10–13).

[1] E-mail: m.bowker@rdg.ac.uk.

2. EXPERIMENTAL

The experimental data were collected using a pulsed flow microreactor built in house and described in full elsewhere (14, 15). The catalyst was composed of one part 5% Rh/γ-Al_2O_3 (Johnson Matthey) mixed with four parts by weight of low surface area α-Al_2O_3 to make a nominal 1% Rh/Al_2O_3; 0.5 g of granulated catalyst was used. Potassium promotion of the pure 5% catalyst was carried out using the incipient wetness technique; 0.25 of a monolayer of potassium was deposited on the catalyst surface.

The catalyst bed is located in a $\frac{1}{4}$-in. o.d. stainless steel U-tube, which itself is housed in a Pye 104 oven, a thermocouple placed in the catalyst bed reads accurate bed temperatures. The temperature ramp employed was linear at 0.5°C/s from 70 to 250°C after which it slowed to 0.4°C/s at 400°C. Immediately prior to the reactor there is a PTFE septum in the $\frac{1}{8}$-in. o.d. stainless-steel line, through which extremely small aliquots of glacial acetic acid (generally 1 μl) were manually injected. The acid vaporized and was carried in the helium stream to the catalyst bed. In test experiments where the gases were diverted through a bypass line, the vaporized acid was detected by the mass spectrometer, indicating that adsorption of acid in the reactor lines was not significant. No acid was detected when it was passed through the catalyst bed. Oxygen pulses (0.5 ml) were dosed into a diluent stream of helium (60 ml per minute) by means of a computer controlled pneumatic valve. The feed gas composition was determined by two six-port valves which can introduce both pulses and continuous flows of different reactant gases to the diluent; these too are pneumatically operated. The postreactor gas line is fitted with a needle valve which allows a small percentage of the gas stream into an on-line quadrupole mass spectrometer for immediate real time product analysis. The time delay between the gases passing over the catalyst bed and being analyzed is ~2 s.

0021-9517/98 $25.00

Before all catalytic tests, a standard procedure was carried out in order to obtain a reproducible catalyst surface. The catalyst was preheated to 400°C under helium then a steady flow of hydrogen at 2 ml per minute was introduced to the diluent flow for 30 min in order to reduce and clean the catalyst from possible organic contamination. The catalyst was cooled under He to 30°C before oxygen and/or acetic acid doses were made.

3. RESULTS

3.1. Oxygen Uptake

The determination of the total metal area of the reduced catalyst was carried out by manually injecting 0.1-ml doses of oxygen gas into the stream of helium via a septum positioned immediately prior to the catalyst bed. The results for both the promoted and unpromoted catalyst are shown in Fig. 1 for several adsorption temperatures. From room temperature up to 100°C the adsorption capacity of the unpromoted catalyst remained essentially constant and saturation was achieved after only two injections, whereas at higher temperatures the uptake was much greater (20 injections, equal to 10 monolayers on the clean Rh/Al_2O_3, were required before full oxygen breakthrough was obtained at 400°C). The metal surface area associated with the uptake at 100°C is 2 $m^2\,g^{-1} \pm (0.2)$, assuming that saturation is 1 : 1 oxygen atoms to surface rhodium atoms and that the surface is of (111) symmetry; thus the area for the 5% $Rh/\gamma\text{-}Al_2O_3$ is 10 m^2/g. This corresponds to a specific metal area of ~200 m^2/g Rh indicating an average Rh particle size of ~20 Å diameter.

The K-promoted catalyst showed a much reduced oxygen uptake indicating blockage of surface sites or reduced metal particle size; the area is reduced by approximately a factor of four.

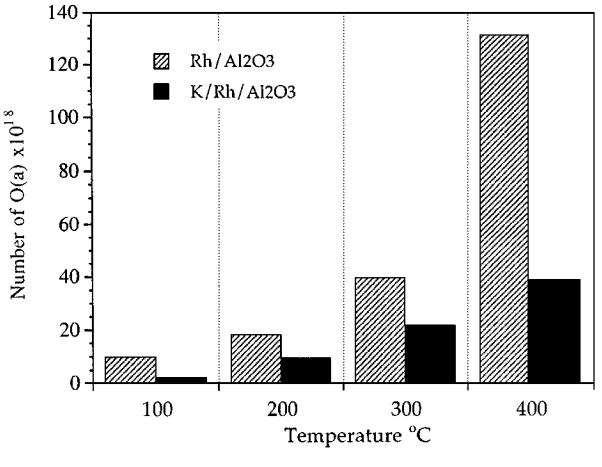

FIG. 1. Oxygen uptake at increasing temperatures over both the potassium-promoted and the unpromoted Rh/Al_2O_3 catalysts.

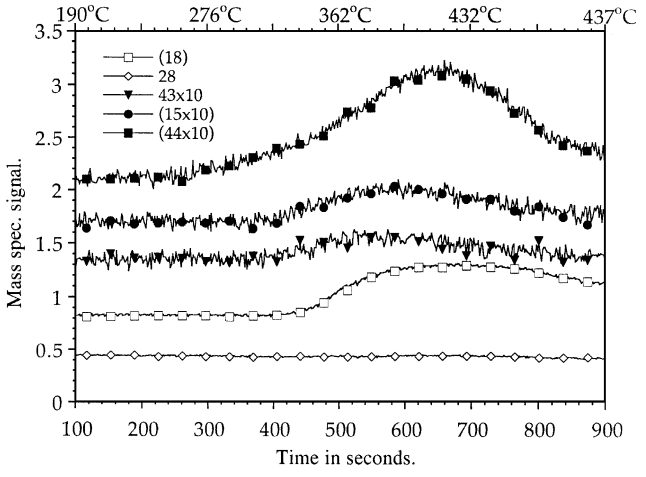

FIG. 2. TPD spectrum after dosing 1 μl of acetic acid onto blank alumina at 100°C.

3.2. Acetic Acid Adsorption on Alumina

Figure 2 shows a TPD experiment after dosing γ-alumina with 1 μl of glacial acetic acid, with the catalyst bed at 100°C. The products are mainly CO_2 and H_2O with smaller amounts of acetic acid (mass 43) and possibly methane, desorbing between 340 and 440°C.

3.3. Acetic Acid Adsorption on Rh/Al_2O_3—No Oxygen Predose

The TPD pattern after acetic acid adsorption on the Rh/Al_2O_3 catalyst is given in Fig. 3. The differences between this and Fig. 2 are severalfold. First, the CO_2 decomposition maximum temperature is lower (appearing at ~340°C opposed to ~400°C). Second, there are prominent CO and CH_4 desorption peaks and the H_2O peak appears at much lower temperatures. Note that the CO and CO_2 desorptions

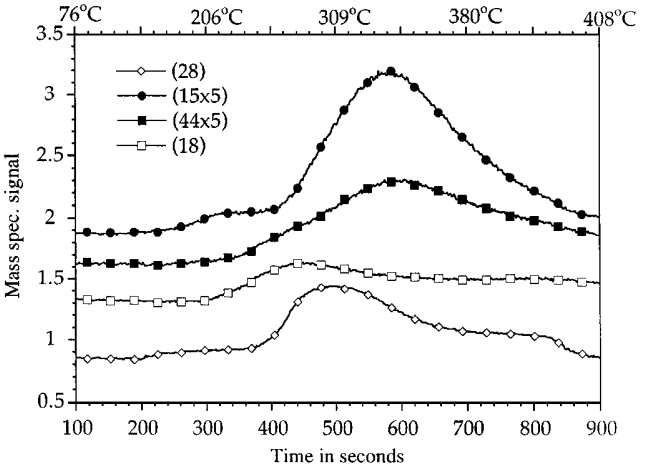

FIG. 3. TPD spectrum after dosing 1 μl of acetic acid onto the Rh/Al_2O_3 catalysts at 50°C.

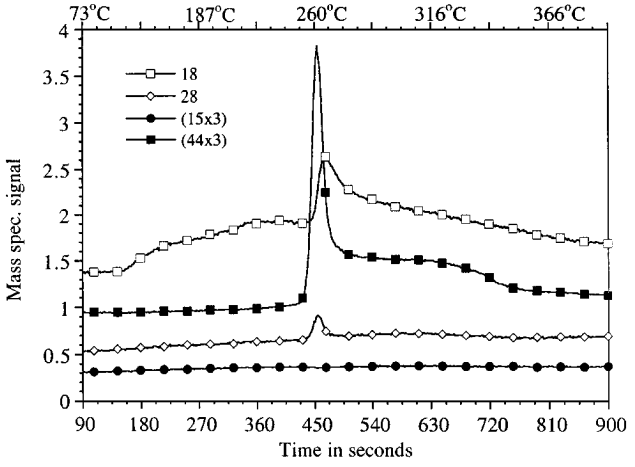

FIG. 4. TPD spectrum showing a well-defined acetate explosion after dosing 0.5 ml O_2 followed by 1 μl of acetic acid onto the Rh/Al_2O_3 catalysts at 50°C.

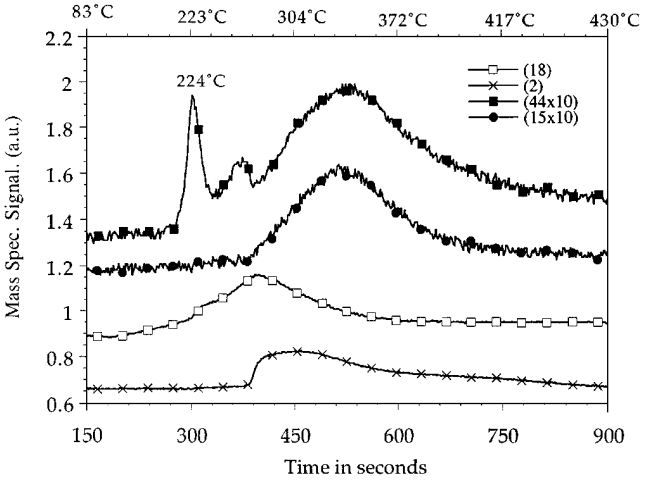

FIG. 6. TPD spectrum showing an acetate explosion followed by H_2 evolution and depleted H_2O production. Experimental regime: 0.1 ml of O_2 followed by 1 μl of acetic acid onto the Rh/Al_2O_3 catalysts at 50°C.

occur with different line shapes indicating that they derive from separate decomposition steps.

3.4. Acetic Acid Adsorption on Rh/Al_2O_3 with Oxygen Predose

Figures 4 and 5 show two examples of desorption spectra after predosing oxygen then acetic acid onto the Rh/Al_2O_3. They show very marked changes in the desorption pattern, with an extremely sharp desorption peak seen for CO_2 at the front end of the CO_2 trace. This type of desorption spectra is characteristic of a so-called "surface explosion," as described in the introduction.

Figure 4 shows the highest temperature "explosive" desorption observed, with an exceptionally clean peak maximizing at ~260°C. Just after the sharp CO_2 peak, a prominent H_2O evolution is seen and is probably associated with the CO_2 desorption but lagged due to readsorption phenomena along the catalyst bed. Figure 5 shows a more typical TPD of acetates from the oxygen precovered catalyst, with the explosion highlighted with shading at the lower temperature end of the spectrum. There is a difference in the higher temperature postexplosion CO_2 desorption pattern with a new peak observed coincident with a water desorption maximising at ~280°C, seen between the two shaded areas, this desorption was not seen in the absence of oxygen predosing. The high-temperature CO_2/CH_4 peak, highlighted in the second shaded area, remains as before (see Fig. 3) as does the CO peak at a slightly lower temperature (280–320°C). There was no significant H_2 production for most oxygen-predosed experiments; however, when a low amount of oxygen was dosed (0.1 ml) as reported in Fig. 6, H_2 was seen between 250 and 350°C and the intermediate CO_2/H_2O peak at ~280°C is seen to abruptly drop off as hydrogen desorption commences.

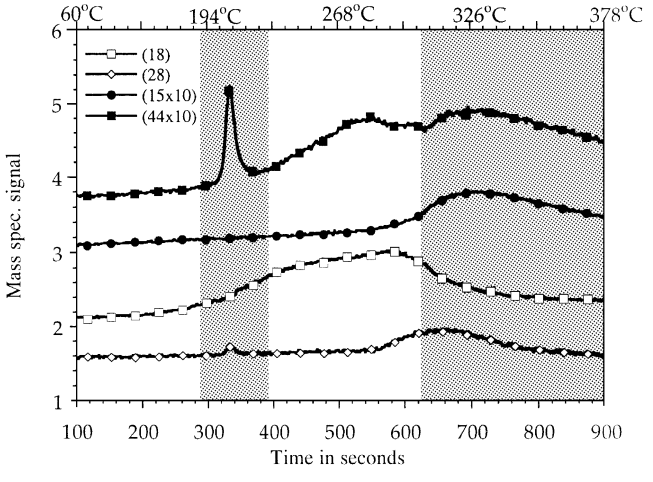

FIG. 5. TPD spectrum showing a more typical acetate explosion showing the higher temperature desorptions due to contributions from acetate species on the support. Experimental regime: 2 ml O_2 followed by 1 μl of acetic acid onto the Rh/Al_2O_3 catalysts at 50°C.

Figure 7a shows the explosive desorption in more detail, demonstrating the autocatalytic nature of the decomposition in a near isothermal experiment. It is demonstrated that the rate increases with time, maximizes, and then decreases to zero as the acetate species is used up. Over the time scale of the experiment (900 s) no desorptions other than CO_2 and H_2O were seen. A second spectrum was taken of the postexplosion catalyst immediately afterward and is shown in Fig. 7b. As the temperature was ramped, the TPD patterns of the more strongly bound species were recorded.

3.5. The Effects of K Promotion

3.5.1. No oxygen predose. The TPD for acetic acid dosed on the reduced catalyst at 100°C is shown in Fig. 8.

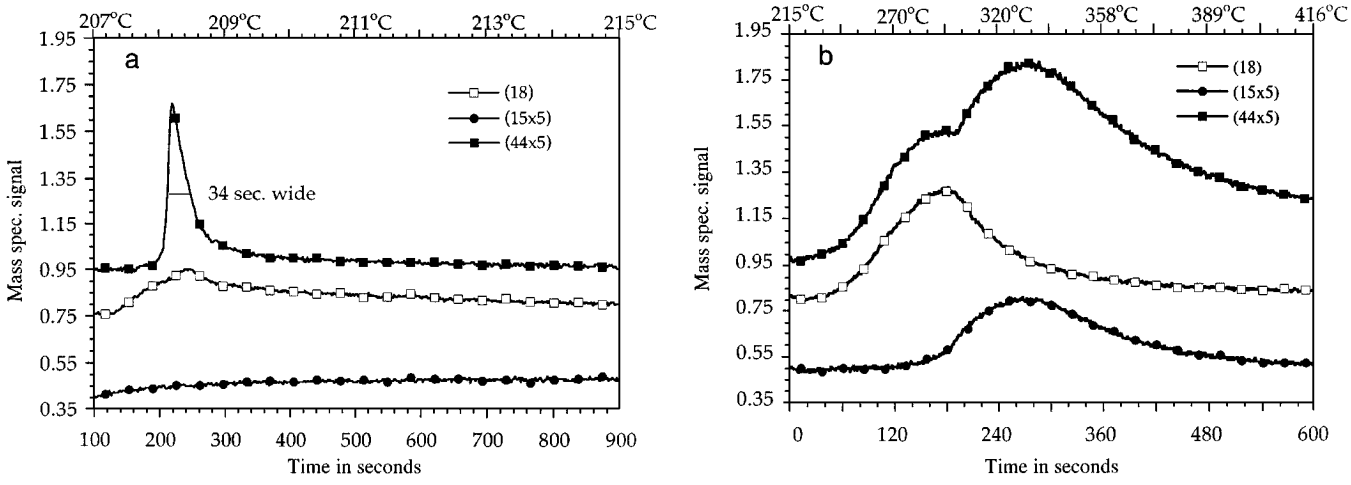

FIG. 7. (a) A near isothermal TPD spectrum revealing the autocatalytic desorption kinetics of the explosive acetates. Experimental regime: 2 ml O_2 followed by 1 μl of acetic acid onto the Rh/Al_2O_3 catalysts at 50°C. (b) TPD spectrum following the explosion seen in (a), revealing in detail the related $CO_2 + H_2O$ and $CO_2 + CH_4$ peaks.

The CO_2/CH_4 peaks associated with decomposition on the support are clearly seen. The major differences between this and the unpromoted catalyst are the larger amounts of CO and H_2 desorbed, evolving coincidentally in two principal peaks at ~320 and ~380°C.

3.5.2. With oxygen predose. With the unpromoted cata lyst, a surface explosion was seen in the TPD spectra after predosing oxygen then dosing acetic acid at ambient temperature (Figs. 4–7). When an identical procedure was followed with the K-promoted catalyst at this temperature (50°C), no explosion was seen. If, however, the dose temperature was increased to 100°C the TPD spectrum displayed in Fig. 9 was obtained, again showing the sharp surface explosion peak. The explosive CO_2 peak is not so sharp as for the unpromoted catalyst and usually appears at a slightly higher temperature (~250°C). Other differences are that there is a broad CO_2 peak occuring before the sharp explosion peak and there appears to be a new H_2O peak starting to desorb at ~170°C which is always associated with this first CO_2 peak. These peaks were not present for oxygen doses of <0.5 ml.

4. DISCUSSION

The desorption spectra shown above are really quite complicated, but an attempt is made here to draw together these

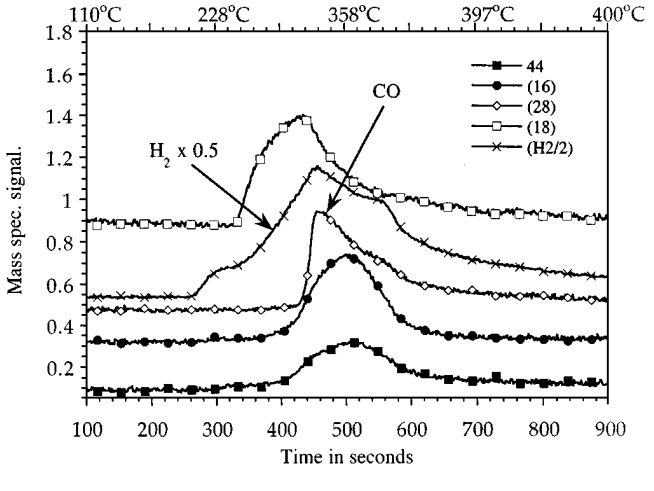

FIG. 8. TPD spectrum after dosing the 0.25 monolayer potassium promoted Rh/Al_2O_3 catalysts with 1 μl of acetic acid at 100°C. Note H_2 and CO desorptions.

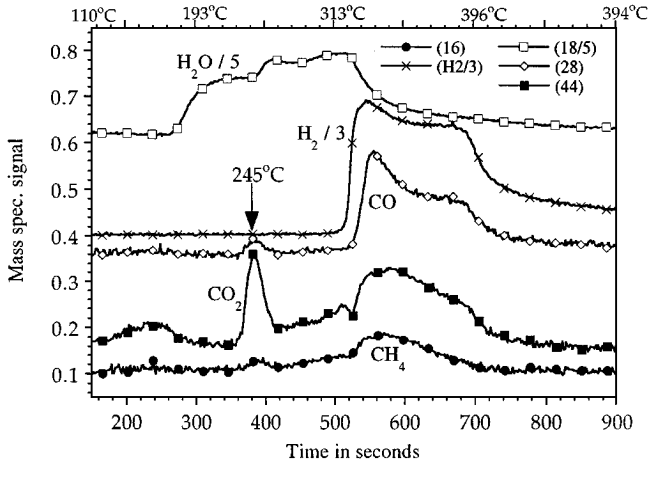

FIG. 9. TPD spectrum after dosing the 0.25 monolayer potassium promoted Rh/Al_2O_3 catalysts with 2 ml of O_2 followed by 1 μ1 of acetic acid at 100°C. Note a broad actetate explosion and new CO_2 and H_2O desorptions at lower temperatures.

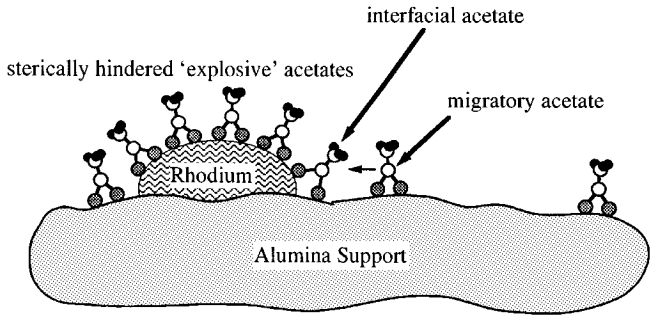

FIG. 10. A model showing a slice through a rhodium particle supported on alumina. The model shows rhodium bound acetates responsible for explosive decomposition, interfacial acetates responsible for $H_2O + CO_2$ desorptions, and support-bound acetate that decompose at higher temperatures to $CH_4 + CO_2$.

observations, with those of others, by using the experience in this group (12, 13, 16, 17) and elsewhere (18) regarding acetic acid adsorption on single crystals. In an earlier publication (5) it was proposed that several types of acetate species could exist on a supported Rh catalyst. This appears to be largely confirmed here and we can propose acetate species associated with the Rh metal, the support, and the interface region. This picture is illustrated more clearly in Fig. 10. Here we show acetates adsorbed on the Rh metal component of the catalyst, in the presence of oxygen atoms, together with acetates on the alumina support and those at the interface of the metal particle/support. Note that all of these species are capable of diffusion, but that the temperature range at which desorption begins is likely to be very different for the differently adsorbed species. The actual shape of the small rhodium particles under reaction conditions is not known—in the model it is illustrated as a pseudospherical entity; however, they could conceivably reconstruct to form flat platelets. It is well known that CO can cause disruption of rhodium particles by the formation of single rhodium dicarbonyl groups. In the case of adsorbed acetate groups, the bond strength is less strong but nevertheless considerable. Let us now proceed with the justification for the model in Fig. 10.

4.1. Acetate on the Support

It is clear from Fig. 2 that acetic acid can adsorb on the support component and that it is relatively stable, decomposing with coincident CO_2 and acetic acid peaks, with maybe some methane, at high temperatures ~340–440°C. Water desorbs slowly from about 310°C, maximizing at ~400°C; no CO desorption occurred.

4.2. Acetate on the Rhodium

Work on single crystals (16, 17) indicates that acetic acid adsorbs dissociatively on Rh as follows.

$$CH_3COOH_{(g)} \rightarrow CH_3COO_{(a)} + H_{(a)}$$

The stability is strongly morphology dependent, the acetate being more stable on the less reactive (111) surface (16). The acetate then decomposes as follows

$$CH_3COO_{(a)} \rightarrow CO_{2(g)} + 3/2\, H_{2(g)} + C_{(a)},$$

leaving carbon on the surface. In the work described here we see no evidence for stable acetate species on the Rh in the absence of an oxygen predose and no evidence for decomposition during gas dosing at ambient temperatures. From single crystal results on Rh it is evident that the presence of oxygen stabilises acetate groups. In our case, as no desorptions are seen during adsorption on the clean rhodium surface, and indeed, the lowest desorption—the surface explosion—occurs when oxygen has been dosed, it appears that in the absence of oxygen, the acetates reside on the alumina. Thus we believe that any acetate species initially adsorbed on the Rh component migrates to the oxide support where it is more strongly bound. Whether this diffusion occurs at the ambient adsorption temperature or during the temperature ramp is not clear.

When oxygen is predosed, then the acetate is stabilized on the rhodium particle and, as found for rhodium single crystals, it decomposes in an explosive fashion, as discussed in more detail below. On the single crystal surfaces the acetate is also stabilized to a considerable degree by oxygen; that is, decomposition occurs at higher temperatures than on a previously clean rhodium surface. This process is morphology dependent, the explosive peak being at ~120°C on Rh(110), with a very narrow peak of 5°C width, whereas on Rh(111) it can appear at temperatures as high as 210°C with a somewhat broader peak width of ~16°C. On the supported catalyst, the peak position is seen between 207 and 260°C and is between 6 and 16°C wide at half peak maximum height.

The stabilization of the acetate on Rh by predosed oxygen was proposed to be due to the blockage of active sites for acetate decomposition by acetate species themselves, either by induced ordering, enhanced coverage or both (13). This can occur by a particular geometrical arrangement of acetates which sterically hinder each other, as shown in Fig. 11. Lower coverages or a more random arrangement leads to defects in the ad-layer (vacancies) which act as decomposition sites. The extrapolation of these ideas to explain the supported rhodium data is now discussed.

On the catalyst we do not have such a regular array of surface atoms as on single crystal surfaces. Thus, it would appear that the explosion is either crucially dependent on the presence of oxygen atoms on the Rh or it is simply due to a high packing density of the intermediates on the surface. The fact that we do not see H_2 evolution coincident with the CO_2 production indicates that oxygen is coadsorbed with the acetate, and, indeed, on single crystal surfaces at very high oxygen coverages no H_2 is evolved with the CO_2; only H_2O is observed (16). In the present study no explosions

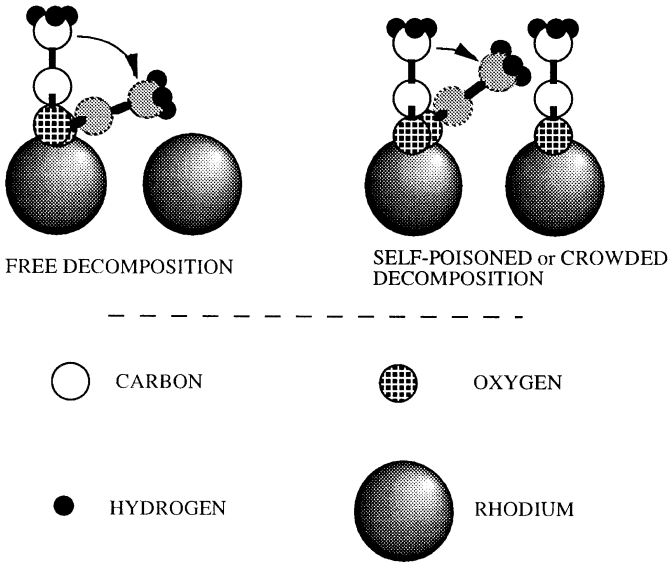

FIG. 11. An illustration of how acetate groups can decompose freely on rhodium or be hindered by steric restrictions. The same adsorbed acetate in a vertical position and (with the carbon atoms shaded) in a bent position prior to decomposition is shown.

were seen in the absence of oxygen dosing; indeed, in that case, the desorption spectra of CO_2 and CH_4 were seen. This was also the case after acetic acid adsorption on blank alumina, suggesting indeed that the acetates are bound to the support, although the ratios are different (more CH_4 than CO_2 in the presence of Rh) suggesting that the presence of rhodium alters the decomposition pathway.

It is clear that the *occurrence* of surface explosions is not morphology dependent for these Rh materials, although the kinetics of decomposition (indicated by the peak width) do vary somewhat with morphology.

4.3. Acetate at the Support–Metal Interface

The data show some evidence for a distinct species which is present at the boundary between the oxygen covered metal and the oxide support. This state we associate with the desorption of CO_2 and H_2O seen at ~280°C in Fig. 5. In the absence of oxygen there is no evidence for this state, which mimics the behavior of the explosive acetate on the Rh in that both CO_2 and H_2O desorb coincidentally. Thus, it is seen in Fig. 5 when oxygen is predosed, but not in Fig. 3 without predosed oxygen. The same applies, although a little less obviously, in the case of the promoted sample (Fig. 8 versus Fig. 9). It would appear that the oxygen located on the metal is helping to anchor the interfacial acetates close to the rhodium. The rationale for their association with the alumina is that they appear at a much higher temperature than the explosive desorption peak, which is from acetate on rhodium, but they also decomposes in a normal nonexplosive fashion. At very low oxygen doses on the unpromoted catalyst there is evidence that this species produces H_2 in its decomposition (Fig. 6), a reaction associated with metal interaction. This indicates, presumably, that at low oxygen coverages, the explosive acetate decomposition uses up the small reservoir of adsorbed oxygen on the rhodium particle, resulting in H_2 evolution from the interfacial acetates, which decompose on the reduced rhodium.

4.4. The Effect of Promotion

Potassium promotion produces a marginal effect on the explosive acetate peak by broadening it. The broadening agrees with recent work by Hoogers *et al.* (18) who examined the effect of acetate decomposition on Rh(111); however, they also found a peak shift to lower temperatures. It must be recognized that the temperature of decomposition of the acetate is higher than in all the single crystal work and the interaction between the coexisting K and O may cause local electronic effects that cause a net stabilizing effect on the acetate group. The higher temperature desorptions are predominantly CO and H_2 rather than CO_2 and water; this is consistent with the reduced oxygen uptake capacity of the promoted catalyst.

5. CONCLUSIONS

It has been shown that acetate groups adsorbed on an alumina-supported rhodium catalyst can decompose in several ways; one pathway can be directly associated with decomposition on the metal and is similar to that on single crystal surfaces. A model has been proposed to explain these observations. When oxygen is predosed onto the catalyst, acetate groups can bind to the $O_{(a)}$/Rh surface and decompose in an explosive fashion, that is, in an autocatalytic reaction. At higher temperatures ~260–310°C, acetates located at the rhodium/support interface decompose to CO_2 and either H_2O or H_2, depending on the availability of $O_{(a)}$. At higher temperatures still, ~320–360°C, acetates adsorbed on the alumina support decompose, probably by migration to Rh centers, as mainly CO_2 and CH_4.

ACKNOWLEDGMENTS

The authors are happy to acknowledge financial support from British Gas and EPSRC for the CASE award to T.J.C.

REFERENCES

1. Bhasin, M. M., Belgian Patent 824, 823, July 28, 1975.
2. Anderson, J. A., and Rochester, C. H., *J. Chem. Soc., Faraday Trans. 1.* **85**(5), 1117 (1989).
3. Burch, R., and Petch, M. I., *Appl. Catal. A: Gen.* **88**, 39 (1992).
4. Houtman, C. J., Brown, N. F., and Barteau, M. A., *J. Catal.* **145**, 7 (1994).
5. Bowker, M., *Catal. Today* **15**, 77 (1992).
6. Ichikawa, M., and Fukushima, T., *J. Chem. Soc., Chem. Commun.* 321 (1985).

7. Bastein, T., Ph.D. thesis, University of Leiden, The Netherlands, 1988.
8. Underwood, R., and Bell, A. T., *J. Catal.* **111**, 392 (1988).
9. Koerts, T., Welters, W., van Santen, R. A., Nonnemann, L., and Ponec, V., *in* "Natural Gas Conversion" (A. Holmen, K. J. Jens, and S. Kolboe, Eds.), *Stud in Surf. Sci. Catal.*, Vol. 61, p. 235. Elsevier, Amsterdam, 1990.
10. McCarthy, J., Falconer, J., and Madix, R. J., *J. Catal.* **30**, 235 (1973).
11. McCarthy, J., Falconer, J., and Madix, R. J., *Surf. Sci.* **42**, 239 (1974).
12. Bowker, M., and Li, Y., *Catal. Lett.* **21**, 321 (1991).
13. Li, Y., and Bowker, M., *J. Catal.* **142**, 630 (1993).
14. Bowker, M., Cassidy, T. J., Ashcroft, A. T., and Cheetham, A. K., *J. Catal.* **143**, 308 (1993).
15. Law, D., and Bowker, M., *Catal. Today* **10**, 397 (1991).
16. Li, Y., and Bowker, M., *Surf. Sci.* **285**, 219 (1993).
17. Aas, N., and Bowker, M., *J. Chem. Soc. Faraday Trans.* **89**(8), 1249 (1993).
18. Hoogers, G., Papageorgopoulos, D. C., Ge, Q., and King, D. A., *Surf. Sci.* **340**, 23 (1995).